Improved out-of-plane material model for metallic honeycomb panels to account for adhesive boundary conditions

Patrick Kendall, Mengqian Sun, Diane Wowk, Christopher Mechefske, Il Yong Kim

Queen's University, Kingston, Ontario, Canada
Royal Military College, Kingston, Ontario, Canada

ARTICLE INFO

Keywords:
Honeycomb
Adhesive
Out-of-Plane
Finite Element Modeling

ABSTRACT

This paper investigates the compressive responses of honeycomb sandwich panels in the out-of-plane direction with attention to the boundary conditions on the top and bottom of the core. When adhesive is added to turn the honeycomb core into a honeycomb sandwich panel, the boundary conditions on the tops and bottoms of the core cell walls change from freely rotating to fixed. This new boundary condition results in a higher peak stress and a lower rebound stress after the plastic collapse. This was further studied by developing a Finite Element model and changing only the boundary conditions to show that it is in fact the fixed boundary condition that alters the loading response. Well known material parameters were utilized to shift key points in a classical material model to fit the experimental curves and provide a bulk material model that better represents a honeycomb panel with adhesive.

Introduction

Honeycomb sandwich structures are heavily used in the aerospace industry due to their excellent stiffness to mass ratio and unique ability to absorb energy in the out-of-plane direction. Regulations on fuel consumption to lessen environmental impact combined with high operational costs are resulting in pressure to make aircraft ever lighter. Honeycomb panels have been accepted in the aerospace industry for use in the fuselage, wing skins and interior components as well as in many other applications. There are still drawbacks to these advanced composites such as impact damage from runway debris, hail, and tool drops, as well as the high level of complexity required to model these structures. The geometric complexity is commonly overcome by means of an equivalent bulk material model that is typically formulated by studying the honeycomb core.

The panels that are studied in this paper consist of an aluminum hexagonal honeycomb core with aluminum face sheets. The face sheets are adhered to the core via structural adhesive that comes in the form of a thin film (Figure 1(a)). The film is baked at 120^0C for 60 minutes for curing, which stiffens the adhesive allowing it to carry high loads. During the curing process the adhesive experiences a drop in viscosity due to the heat and migrates up the honeycomb cell walls due to surface tension to form what is called an adhesive fillet. The adhesive fillet is strived for in the manufacturing process and is believed to improve bonding between the face sheet and the core [1]. This paper will examine how the adhesive constrains motions and rotations at the top and bottom of the core and how it affects the stress strain response in the out-of-plane direction.

Honeycomb panels are complex structures with complex interior geometry which can make the modelling and simulation process difficult. The tiny repeating cells throughout the panels call for a fine mesh and, in turn, a computationally expensive model. To tackle this problem, engineers use what is called a homogeneous modelling technique [2][3]. This technique works under the assumption that complex continuous geometries can be modelled as a solid bulk material that is calibrated to behave in the same manner as their detailed counterparts. This is done with honeycomb by referencing an orthotropic material model that represents the loading response in shear, compression, and tension in each direction. Considering that honeycomb panels are such a heavily used component, there are pre-

existing equations that can provide a user with a material model based on the metallic material used to make the core and the specific dimensions of the hexagonal cells (Equations (1)-(3)). This paper will only be concerned with the out-of-plane compression response in the material model.

Researchers in the field of metallic honeycomb have developed equations to describe the out-of-plane compression behaviour that can be calculated using the geometry found in the honeycomb core (Figure 1 (b)). McFarland began to study the hexagonal cellular solids out-of-plane loading response by building a semi-empirical expression for the plateau stress, which is the constant load that the honeycomb undergoes during post buckling [4]. Weirzbicki furthered this research by accounting for the double cell walls in honeycomb core and improving the prediction of the plateau stress [5]. The double cell walls are a result of the manufacturing process called honeycomb expansion. Gibson and Ashby [6], and Zhang and Ashby [7] advanced this field of study by adding expressions for peak stress as well as summarizing the material properties in all directions, including shear.

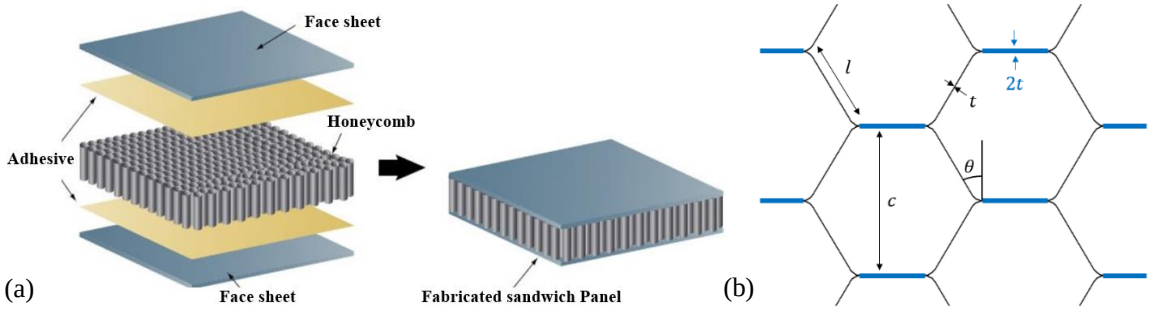

Figure 1: (a) Layering in the manufacturing process for honeycomb panels. (b) Dimensions used to formulate out-of-plane compression material models (double cell walls highlighted in blue).

From the literature review, a material model of the honeycomb core was built by utilizing Equations (1)-(3). These equations were extracted from publications by the authors mentioned above [5][6][7]. Parameters used in the equations are the elastic modulus of the material used (E_s), the thickness of the cell walls (t), the length of each cell wall (l), the poisson's ratio of the material used (ν_s), the angle at the edges of the hexagonal cells (θ), and the yield stress of the material (σ_{ys}). The value K in the equation for peak stress (σ_{pk}) is given a value of 5.73 and is related to the side constraints assumed for neighbouring cells. The K value is described in more detail in Zhang and Ashby [7]. A generalized representation of the material model can be found illustrated in Figure 2. The out-of-plane direction has gained much attention in the literature due to the energy absorption properties as well as the complexity in the buckling failure mechanisms [8][9][10].

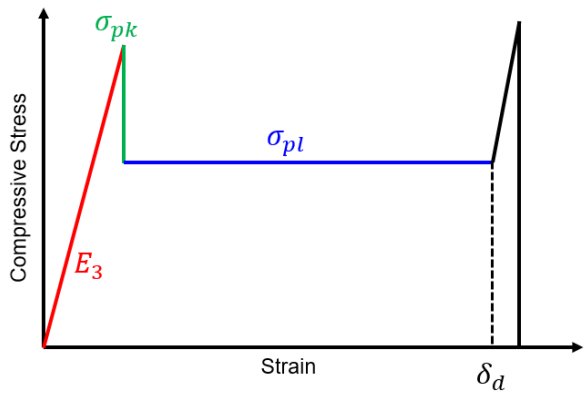

$$E_3 = E_s\left(\frac{t}{l}\right) \quad (1)$$

$$\sigma_{pk} = E_s\left(\frac{5K}{\left(1-\nu_s^2\right)cos\theta\left(1+sin\theta\right)}\left(\frac{t}{l}\right)^3\right) \quad (2)$$

$$\sigma_{pl} = 6.6\sigma_{ys}\left(\frac{t}{l}\right)^{5/3} \quad (3)$$

Figure 2: Generalized graphical representation of the classical out-of-plane material model for a honeycomb core.

The classical material model is idealised for a honeycomb core and is implemented into FE modelling by adding metallic or composite face sheets to either end. This paper will look to improve the classical material model by

completing out-of-plane compression experiments on assembled panels with adhesive and face sheets. The expectation is that the adhesive fillets provide a significant bracing effect to the cell walls, which restricts the translational motion and rotation at the top or bottom edges of the honeycomb core. This will therefore change the boundary condition found in honeycomb core experiments from freely rotating to fully fixed. The fixed boundary condition is something that some researchers employ in their modelling process [11][12][13], while others simply share nodes at the interface [14], or use tie constraints [15][16][17]. However, homogeneous modeling techniques are not concerned with the nodal connections at the cell walls and use material models based on honeycomb core with no face sheets or adhesive. This paper will look to build a new material model based on experimental data that considers the adhesive effects on the honeycomb core to increase the accuracy of homogeneous material model. The material model will be an extension of the current model and no new parameters will need to be calculated.

Materials and Methods

The adhesive study was carried out by manufacturing three honeycomb panels and comparing their out-of-plane compression responses to a honeycomb core that underwent the same test. The resulting data was compared to the classical material model as well as the honeycomb core control test to observe any discrepancies. Once the key differences were identified the buckling mechanisms were investigated around these data to discover the physical cause of the discrepancies. The material model was then adjusted to improve the quality of fit to the experimental data to better represent a real world panel.

Materials

The panels were manufactured by adhering two 0.5mm thick aluminum face sheets on either side of an aluminum honeycomb core using a structural adhesive film. The aluminum used for the core was 5052 H38, which has an Elastic Modulus of 71 GPa, a yield strength of 345 MPa and a Poisson's ratio of 0.3. The 12mm thick core has a cell size (l) of 1.83mm and a cell wall thickness (t) of 0.02mm (Figure 1(b)). The material properties for the aluminum as well as the core geometry serve as the input values for the classical material model (Equations (1)-(3)).

Specimens

The adhesive film was cured on a heat bed at 120^0C for 60min. The heat bed was ramped up and down at 1^0C/min. During this process the adhesive film experiences a drop in viscosity due to the temperature increase which enables it to migrate up the cell walls due to surface tension. During the ramp down process the adhesive retains its final shape which is in the form a fillet along the edge of the cell walls (Figure 3).

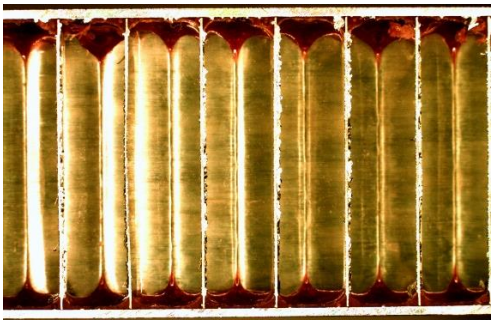

Figure 3: Adhesive fillets (shown in red) found in the manufactured panels.

Experimental Procedure

The panels and honeycomb core were then compressed using an Instron testing machine where the core and panels were loaded at a rate of 1mm/min to avoid any strain rate effects. See Figure 4 for an illustration of the test set up. Buckling initiated in the honeycomb core at the top and bottom of the cell walls while the buckling initiated in the honeycomb panels at a random position along the thickness of the core between neighbouring cells. This is discussed in more detail in the results and discussion section. The measurements from the Instron testing machine load cell were converted to compressive normal stress by dividing by the area of the coupon being tested. The compression stroke

of the machine was also represented as strain by dividing the stroke of the machine by the original thickness of the coupon.

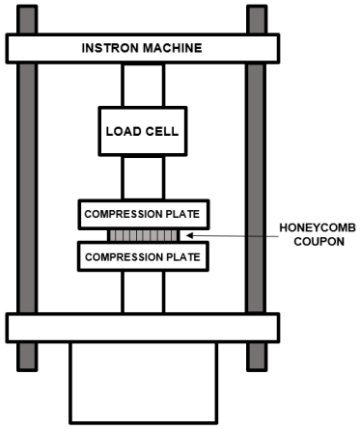

Figure 4: Instron Testing Machine set up for out-of-plane compression tests.

Computational Procedure

A numerical model was prepared in HyperWorks Radioss and compared with experimental findings. The model consisted of six unit cells made up of 2D shell elements. Shell elements along the ribbon direction were given a double thickness to simulate the double walls produced from honeycomb expansion. All top nodes moved with the same prescribed displacement in the third principal direction, while all other directions were constrained. The translation and rotation of the outer most nodes in the model were constrained to prevent motion along the cell wall to simulate symmetry and represent an infinite honeycomb. A rigid surface with a general contact definition was used between the honeycomb and rigid wall. The top nodes were displaced in the out-of-plane in the out-of-plane direction causing plastic collapse through buckling to occur in the model. The material model used for the 5052 H38 aluminum core was assumed to be elastic perfectly plastic. Two models were built for this study. The first model was built with no constraints on the base nodes that contacted the rigid wall so the nodes were free to translate or rotate and the second model was given a fixed constraint at the base nodes that contact the rigid wall. The goal of the computational model is to study the effects of the boundary conditions rather than stress prediction. When adhesive is added to the honeycomb core, thus making it a panel, the end conditions were expected to behave as though they were fixed. The FEA was used to isolate the boundary condition to show how it affects the out-of-plane properties.

Results and Discussion

Three honeycomb cores and three honeycomb panels were compressed and each data set showed excellent repeatability between tests. For this reason, only one set of data will be examined for the honeycomb core as well as the panel. The data sets were compared to the calculated classical material model given the honeycomb core used for the experiments. The resulting values for the classical material model can be found in Table 1.

Table 1: Calculated material model for comparison with experimental results.

Material Model Parameter	Calculated Value
Elastic Modulus (E_3)	658.50 MPa
Peak Stress (σ_{pk})	1.60 MPa
Plateau Stress (σ_{pl})	1.09 MPa

Honeycomb Core

Buckling initiated in the honeycomb core at the top of the cell walls where the boundary condition was free to translate and rotate. This happened with each coupon and was deemed to be a path of least resistance when it came to plastic collapse through buckling. Following the plastic collapse at the peak stress, a continuous buckling mechanism took

place as each fold was sequentially formed until full densification. Figure 5(a) shows the folding pattern found in the cross sectioned core. The wavy pattern of the buckling failure in the core can be seen in the resulting stress strain data collected from the load cell and stroke of the Instron testing machine as the oscillations occur about a plateau stress (Figure 5(b)). The classical material model is overlaid on the experimental data to show a linear section leading to a peak stress and falling to a plateau stress. The data shows misalignment with the material model at the beginning of the data. This is because the elastic modulus is measured by the linear section of the experimental data and the sloping curve at the beginning of the test can be omitted. See the ASTM standard for flatwise compression of a honeycomb core for more details [18]. The experimental data, although less linear and sudden, show a peak stress of 1.78 MPa (11% higher than the calculated value) that falls towards a plateau stress.

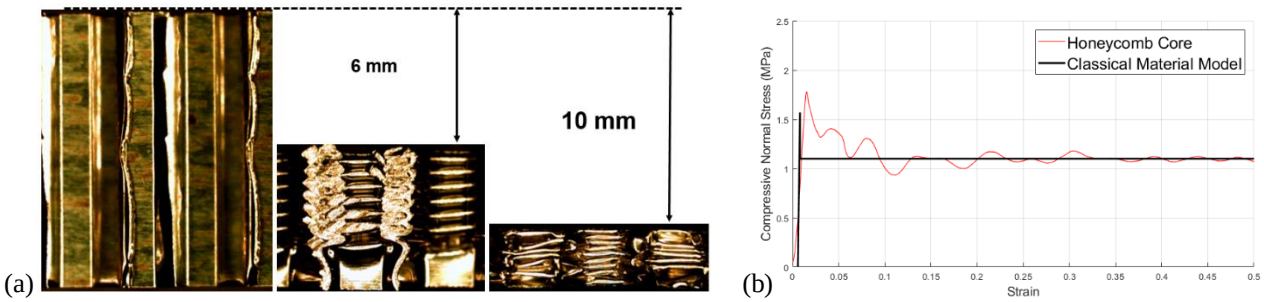

Figure 5: (a) Out-of-plane compression response of honeycomb core. (b) Honeycomb core compression data compared with the classical material model formulated from Equations (1)-(3).

Honeycomb Panel

Buckling initiated in the honeycomb panel at random locations for each unit cell and the adhesive was able to constrain the cell walls that it encompassed (Figure 6(a)). Each coupon showed a unique buckling location for the first fold, which suggests that the adhesive increases the level of difficulty when it comes to predicting failure in the core. The peak stress was found to be 2.4 MPa which is 50% higher than that of the calculated peak value from the classical material model of 1.6 MPa. There was a new section to the curve that was observed after the plastic collapse. The rebound towards the plateau stress is much more severe in the honeycomb panel and produces stresses even lower than the plateau to a value of 0.68 MPa which is approximately 33% lower than the plateau. This event is only observed in the first buckling fold and initial collapse and then the stress rises and remains at the plateau stress until densification. All of these trends can be found in Figure 6(b) where the experimental data for the panel is compared with the classical material model. This highlights the key differences and unique loading responses that are not captured by the classical material model.

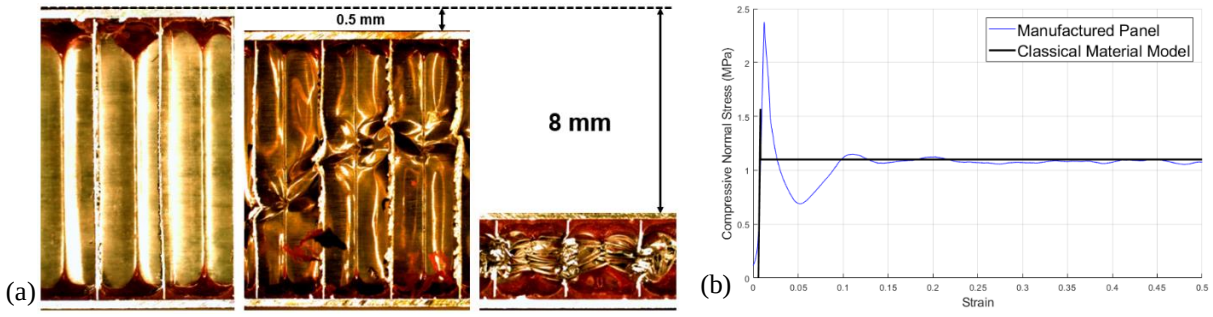

Figure 6: (a) Out-of-plane compression response of honeycomb panel. (b) Honeycomb panel data compared with the classical material model formulated from Equations (1)-(3).

Computational Results

The previous section showed a significantly higher peak stress in the honeycomb panel when compared with the honeycomb core at a value of approximately 3/2 times that of the calculated peak of 1.57 MPa. This higher peak stress

is a result of the different boundary conditions between the honeycomb core and honeycomb panel coupons. The honeycomb panels are constrained on the top and bottom by the structural adhesive, thus providing the edges with a fixed boundary condition, while the honeycomb core has no such constraint and can be considered as a free boundary condition in contact with the compression plates. This alters the buckling mechanisms as well as the onset of instability. The plastic collapse location can always be predicted in a honeycomb core as either the top or bottom of the honeycomb at the cell wall free boundary. This is because the free edges have the ability to rotate and translate (slightly), providing a path of least resistance for the first plastic hinge to form. Figure 7 shows a "Y" shape model of a honeycomb core with a free boundary condition under displacement controlled out-of-plane compression. This was used to show the folding pattern with a fine mesh. The ability for the base nodes to rotate and translate, just like a honeycomb core compression test, results in the same failure mode in each simulation. The fixed boundary condition was implemented in a larger six cell model and shows a much less predictable pattern of plasticity through the height of the structure by constraining the location of the initial buckle. By removing the path of least resistance caused by the free boundary condition from the compression test, the critical load to cause buckling increases.

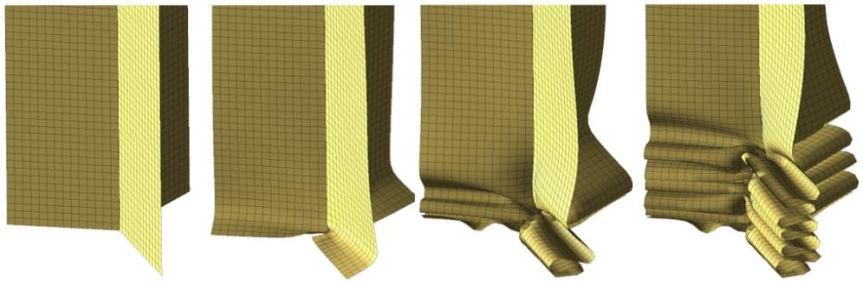

Figure 7: "Y" shape model with free boundary conditions illustrates the onset of plastic buckling beginning at the base nodes.

The experimental results showed the onset of buckling beginning at random heights between neighbouring unit cells. To study this finding in HyperWorks, the model described in the computational methods section was utilised to view how the boundary conditions can affect the location of the first plastic hinge given each of the six cells. The resulting stress strain response from the fixed boundary condition was consistent with experimental data for the honeycomb panels and produced an unpredictable initial collapse location at a higher stress than the free boundary condition.

The change in boundary condition also creates a lower rebound in the plateau stress soon after the peak stress is reached. This lower rebound is due to the added resistance in forming the second fold in the buckling process, while the honeycomb core is able to form sequential folds and remain at the plateau stress. Figure 8 (a) and (b) shows the core and panel cross sections of the computational results while they move through the various stages in the compression stroke in comparison with experimental images to show the validity of the FEA. The model was used to get a closer look at the interior buckling modes during loading and to draw conclusions about the changes in failure modes given the new boundary conditions. It was observed in the model that the honeycomb core forms new folds continuously before the first has completely collapsed, while the honeycomb panel brings the first fold to a full compression before exhibiting a continuous buckling mechanism. The first fold appears to be larger in wavelength in the honeycomb panel when compared to the honeycomb core, which could be a result of the added resistance to buckling caused by the fixed boundary conditions. Figure 8 (b) furthers the comparison by showing correlations between the experimental load cell data for the honeycomb core and the reaction forces calculated at the rigid node in the free boundary condition model. All results were converted to stress and strain values for the comparison. The same process was done with experimental data for the manufactured panel and the fixed boundary condition model. The main finding in this computational study is that the higher peak stress is found in both the honeycomb panel data and the fixed boundary condition results, as well as the severe rebound after plastic collapse.

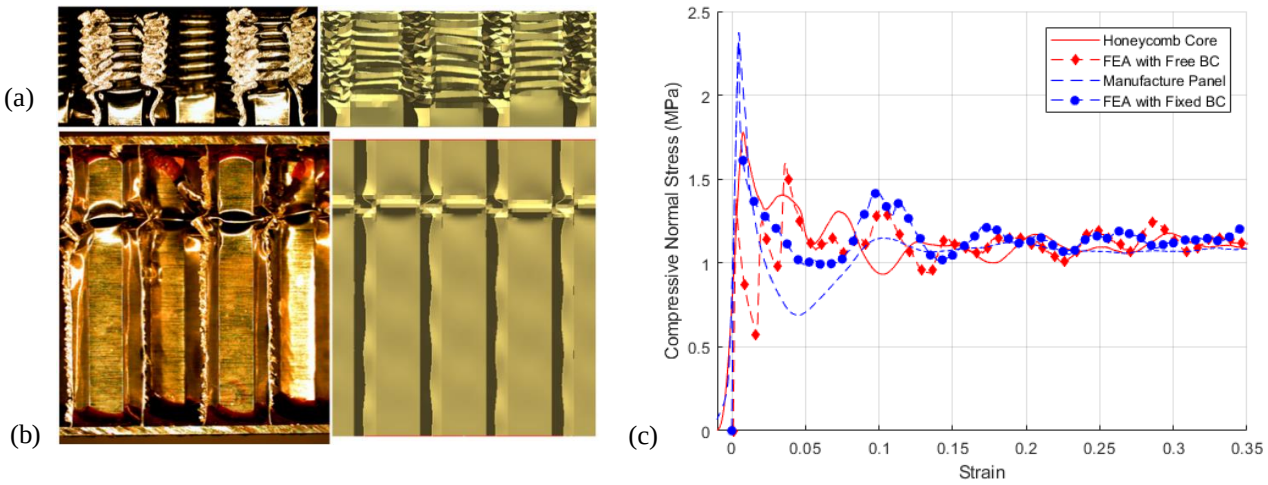

Figure 8: (a) Visual comparison between partially compressed honeycomb core and the free boundary condition model. (b) Visual comparison between partially compressed honeycomb panel and the fixed boundary condition model. (c) Experimental data from the honeycomb core and panel compared with numerical results with free and fixed boundary conditions.

Material Model Formulation

In order to represent the real world response of the honeycomb panel, some adjustments were introduced to the material curve to account for new boundary conditions and the various effects it has on the loading response. These adjustments were derived based on patterns found in the experimental results. The peak stress increased when the boundary condition was changed from free to fixed at the top and bottom of the honeycomb. The increase was constant given all experimental tests, therefore the adjustment was made by scaling the originally calculated peak stress to a point that better matched the experimental results. The rebound after buckling collapse of the honeycomb reached a stress value lower than the plateau stress, which has not been accounted for in the classical material model. The adjustments to the material model to account for this were made by approximating the section between the peak and plateau stress as a quadratic equation and a straight line. The new material model was fit by taking three points that were consistent in all the experimental data sets and representing them in terms of the Elastic Modulus, peak stress and plateau stress (Figure 9). These parameters can be calculated given Equations (1)-(3) and depend on the honeycomb geometry and aluminum material properties. The new scaled points were then used to fit a combination of linear and curve-a-linear functions to give an accurate representation of the experimental results. These formulations can be found in the new material model shown as a piecewise function in Equation (4) where x represents strain and $f(x)$ represents stress. The proposed material model calculates values until the densification of the honeycomb core, which was found experimentally at 0.85 strain. The densification stage has had little attention in the literature and a published equation for calculating the strain value at which it occurs could not been found. The curve produced from the new material model can be seen overlaid on the experimental data collected from the manufactured panel in Figure 10.

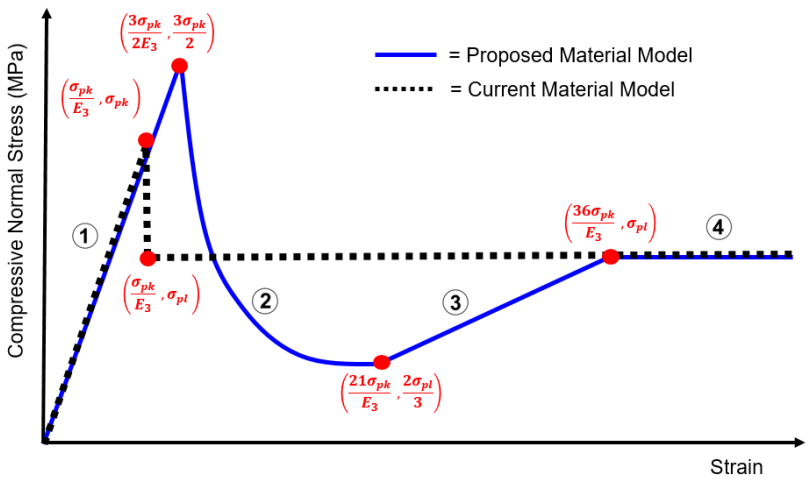

Figure 9: Proposed material model built from three coordinates. Sections (1), (3) and (4) are represented as linear functions while (2) is formulated as a quadratic.

$$f(x)=\begin{cases} E_3 x & \text{if} \quad 0 \le x \le \dfrac{3\sigma_{pk}}{2E_3} \quad (1) \\ \dfrac{E_3^{\,2}}{\sigma_{pk}}\left(0.004-0.002\dfrac{\sigma_{pl}}{\sigma_{pk}}\right)\left(x-\dfrac{21\sigma_{pk}}{E_3}\right)^2+\dfrac{2\sigma_{pl}}{3} & \text{if} \quad \dfrac{3\sigma_{pk}}{2E_3} \le x \le \dfrac{21\sigma_{pk}}{E_3} \quad (2) \\ \dfrac{E_3\sigma_{pl}}{45\sigma_{pk}}x+\dfrac{\sigma_{pl}}{5} & \text{if} \quad \dfrac{21\sigma_{pk}}{E_3} \le x \le \dfrac{36\sigma_{pk}}{E_3} \quad (3) \\ \sigma_{pl} & \text{if} \quad \dfrac{36\sigma_{pk}}{E_3} \le \mathrm{x} \le 0.85 \quad (4) \end{cases} \tag{4}$$

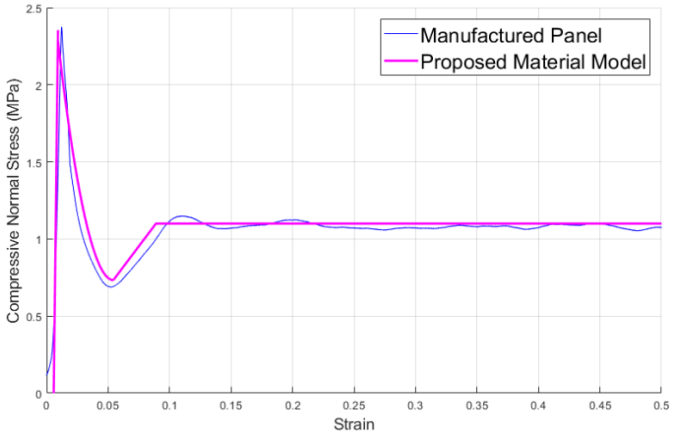

Figure 10: New material model compared with experimental out-of-plane compression data for honeycomb panel.

Conclusions

The changes in honeycomb cell wall boundary conditions, given the introduction of structural adhesive, have a direct effect on the out-of-plane compression behaviour of aluminum honeycomb sandwich structures. The new boundary condition affects the formation of the initial local deformation and thus produces inconsistencies between honeycomb

core and honeycomb panel in the form of stress values below the plateau after the buckling collapse which happens at the peak stress. This behaviour was effectively modelled with the use of Hyperworks to confirm that it is in fact the changing boundary condition that causes this behaviour. A new material model was formulated by means of curve fitting to provide a more accurate representation of a real world panel.

This paper adds to the literature with respect to the adhesive effects and adds to the current understanding of out-of-plane compressive behaviour. The presented study advances the research in the damage resistance of aluminum honeycomb panels and leads to a better homogeneous model of advanced composites. Engineers and researchers can utilise the new material model to conduct homogeneous modelling practices with a high level of certainty in the results.

Acknowledgments

This research was funded by the Natural Sciences and Engineering Research Council of Canada (NSERC) and National Defense Canada. Technical advice was gratefully received from Dr. Ross Underhill, Dr. David DuQuesnay, and Mr. Tanner Rellinger of the Royal Military College of Canada. This research could not have been possible without the support and collaboration of the Structural and Multidisciplinary Systems Design Group at Queen's University.

Reference

[1] R. T. B. Keith B. Armstrong, *Care and Repair of Advanced Composites*. warrendale, PA: Society of Automotive Engineers, Inc, 1998.

[2] A. M. Wagih, M. M. Hegaze, and M. A. Kamel, "FE modeling of Satellite's Honeycomb Sandwich Panels Using Shell Approach and Solid Approach," no. September, 2017.

[3] M. Modeling, S. Heimbs, P. Middendorf, and M. Maier, "Honeycomb Sandwich Material Modeling for Dynamic Simulations of Aircraft Interior Components," pp. 1–13.

[4] R. K. MC FARLAND, "Hexagonal Cell Structures Under Post-Buckling Axial Load," *AIAA J.*, vol. 1, no. 6, pp. 1380–1385, 2008.

[5] T. Wierzbicki, "Crushing analysis of metal honeycombs," *Int. J. Impact Eng.*, vol. 1, no. 2, pp. 157–174, 1983.

[6] L. J. G. and M. F. Ashby, *Cellular solids, Structures and properties - Second edition*, Second. Cambridge University Press, 1997.

[7] J. Zhang and M. F. Ashby, "The out-of-plane properties of honeycombs," *Int. J. Mech. Sci.*, vol. 34, no. 6, pp. 475–489, 1992.

[8] A. S. M. Ashab, D. Ruan, G. Lu, S. Xu, and C. Wen, "Experimental investigation of the mechanical behavior of aluminum honeycombs under quasi-static and dynamic indentation," *Mater. Des.*, vol. 74, pp. 138–149, 2015.

[9] I. Ivañez, L. M. Fernandez-cañadas, and S. Sanchez-saez, "Compressive deformation and energy-absorption capability of aluminium honeycomb core," vol. 174, pp. 123–133, 2017.

[10] Z. Bai, H. Guo, B. Jiang, F. Zhu, and L. Cao, "Thin-Walled Structures A study on the mean crushing strength of hexagonal multi-cell thin-walled structures," *Thin Walled Struct.*, vol. 80, pp. 38–45, 2014.

[11] D. Zhang, D. Jiang, Q. Fei, and S. Wu, "Experimental and numerical investigation on indentation and energy absorption of a honeycomb sandwich panel under low-velocity impact," *Finite Elem. Anal. Des.*, vol. 117–118, pp. 21–30, 2016.

[12] T. Umeda and K. Mimura, "Effects of boundary condition and cell structure on dynamic axial

crushing honeycomb," vol. 5, no. 2, pp. 1–11, 2018.

[13] Y. Aminanda, A. G. E. Sutjipto, E. Y. T. Adesta, and B. Castanie, "Simulation of Compression and Spring-back Phenomena of Sandwich Structure with Honeycomb Core Subjected to Low Energy and Low Velocity Impact," *Fract. Strength Solids Vii, Pts 1 2*, vol. 462–463, pp. 1296–1301, 2011.

[14] Y. Chen, S. Hou, K. Fu, X. Han, and L. Ye, "Low-velocity impact response of composite sandwich structures: Modelling and experiment," *Compos. Struct.*, vol. 168, pp. 322–334, 2017.

[15] C. C. Foo, L. K. Seah, and G. B. Chai, "Low-velocity impact failure of aluminium honeycomb sandwich panels," vol. 85, pp. 20–28, 2008.

[16] L. Liu, H. Feng, H. Tang, and Z. Guan, "Impact resistance of Nomex honeycomb sandwich structures with thin fibre reinforced polymer facesheets," 2018.

[17] Z. Xie, W. Zhao, X. Wang, J. Hang, X. Yue, and X. Zhou, "Low-velocity impact behaviour of titanium honeycomb sandwich structures," 2018.

[18] C. Materials and ASTM, "Standard Test Method for Flatwise Compressive Properties of Sandwich Cores 1," *Current*, vol. i, pp. 2–4, 2003.